

# Coherent ecological dynamics induced by large scale disturbance

Timothy H. Keitt, Integrative Biology, University of Texas, Austin, Texas 78712 USA

## Supplementary Figures

**Alternative analysis of seasonal biomass dynamics.** To further explore seasonal phase shifts in the LRL data, I analyzed species specific and total biomass as a function of day-of-year during three different time periods. Figure S1 shows scatter-plot smooths of log+1 transformed biomass versus day-of-year. Smoothing was accomplished by fitting a smoothing spline to each species scatter plot and to the biomass summed across species. The `smooth.spline` function from  $R^1$  was used with residual degrees of freedom set at 16. Periodic boundary conditions were enforced by adding two extra copies of the data, one to the left side of the plot with 365 subtracted from the day-of-year and another added to the right with 365 added to the day-of-year. The additional copies were then removed from the final output.

The period of greatest interest is 1990-1994 (middle column), roughly the interval during which the wavelet method detected a significant difference between reference and treatment basins. The period preceding and following this interval are included for comparison. Notice the strong seasonal oscillation in total biomass in the treatment basin. Biomass peaks during summer and drops to a minimum during the spring. Total biomass is relatively constant by comparison in the reference basin during this period. The dramatic reduction in biomass and shift in seasonality of the acid sensitive species *Leptodiptomus* (bright yellow) and *Diacyclops* (black) are clearly evident in the treatment basin.

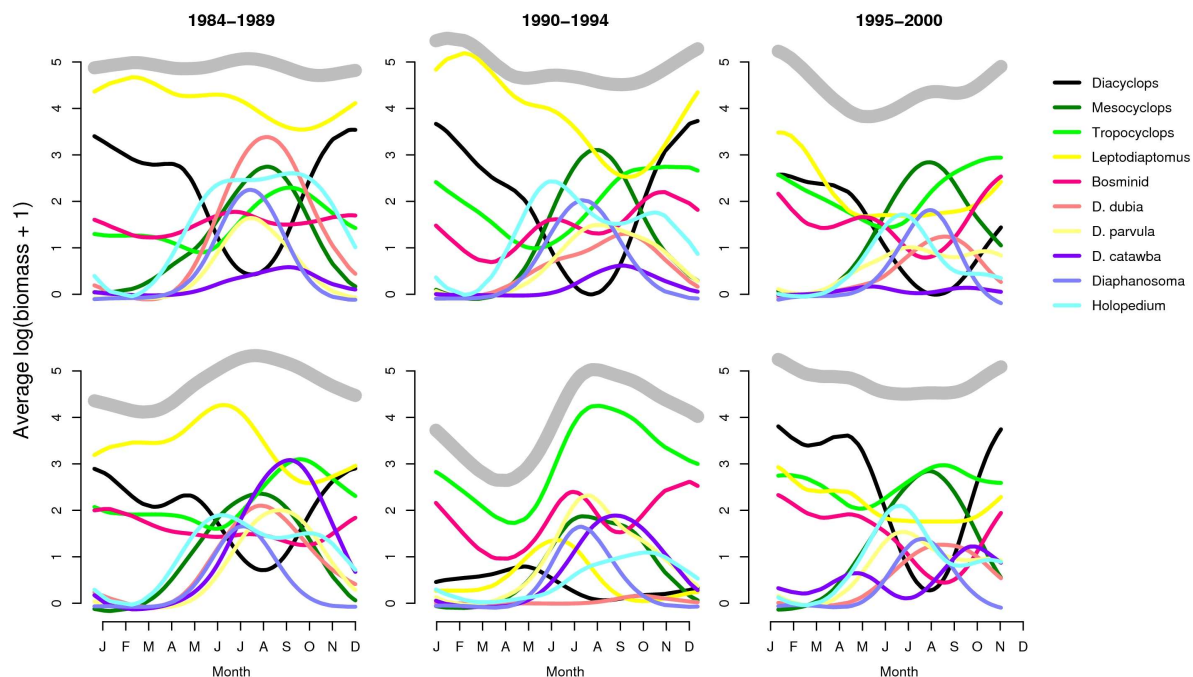


Figure S1: Seasonal variation in biomass during three phases of the acidification experiment (reference: top row, treatment: bottom row). Curves are scatter plot smooths of the log-transformed biomass versus day-of-year for each species. The thick grey line tracks seasonal variation in total biomass.

**Applications to simulated data.** I evaluate the ability of the wavelet modulus ratio to detect synchronous

and compensatory patterns via Monte Carlo studies. Artificial time series were simulated using a periodic multivariate autoregressive model given by

$$x_i(t) = \alpha_i + \sum_{j=1}^N \beta_{ij} x_j(t-1) + \gamma_i \cos(2\pi t + \delta_i) + \sigma \epsilon(t) \quad (1)$$

where  $x_i$  is the log-transformed biomass of the  $i$ th species,  $\alpha_i$  is the intrinsic growth rate of species  $i$ ,  $\beta_{ij}$  models the effect of species  $j$ 's biomass on species  $i$ ,  $\gamma_i$  is the amplitude of the seasonal growth component,  $\delta_i$  is the seasonal phase determining the timing of peak abundance, and  $\epsilon(t)$  are normally distributed environmental perturbations with variance  $\sigma^2$ . This model is equivalent to a log-transformed Gompertz density-dependent community model,<sup>2</sup> albeit with an added seasonal component. A comprehensive analysis of the model is beyond the scope of this supplement and will be presented elsewhere. For the purposes of this study, I ignored species interactions by setting  $\beta_{ii} = -0.1$  and  $\beta_{ij} = 0.0$  when  $i \neq j$ . I also ignored variation in vital rates among species. Parameters for all 10 simulated species were set to  $\alpha = 1, \gamma = 1$ , and  $\sigma = 0.1$ . Species seasonal phases varied individually according to three scenarios: 1)  $\delta_i \sim \text{Uniform}(-\pi, \pi)$  i.e. no pattern, 2)  $\delta_i \sim \text{VonMises}(0, \kappa)$  giving a mean phase of 0 and phases concentrated according to  $\kappa$  (the VonMises distribution is the angular equivalent of the normal distribution where  $\kappa$  is analogous to the inverse standard deviation<sup>3</sup>), and 3) the first 5 species  $\delta_i \sim \text{VonMises}(0, \kappa)$  and the second 5 species  $\delta_i \sim \text{VonMises}(\pi, \kappa)$ . Scenario 2 produces synchronous dynamics as  $\kappa$  grows large whereas scenario 3 generates compensatory dynamics as  $\kappa$  increases. In all cases, analysis was restricted to the annual time scale.

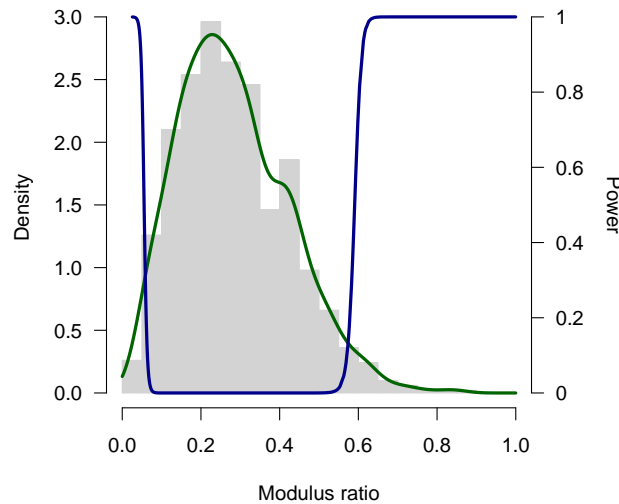


Figure S2: Estimated probability density of modulus ratios (dark green) obtained under scenario 1 (uniform random phases) and frequency of rejecting the two-tailed null hypothesis of no pattern using the phase perturbation method (see main text). The density line is a kernel-density estimate.<sup>4</sup> Detection probability (power) was estimated using a binomial local regression model<sup>5</sup> fit to results of 1000 simulations equally split between scenarios 2 and 3.

Figure S2 shows results from 2000 simulations of the model using parameters described previously. In the first set of 1000 simulations, scenario 1 was used to generate species phases. These data were used to compute the expected probability density of modulus ratios when species phases are distributed uniformly on the circle. In the second set of 1000 simulations, phases were split evenly between scenarios 2 and 3. In both cases,  $\kappa \sim 10^{\text{Uniform}(-3,3)}$  resulting in values spanning from uniform on the circle ( $\kappa = 0.001$ ) to highly concentrated ( $\kappa = 1000$ ). The model was iterated 300 times and then simulated an additional 300 steps spanning 17 seasons. The modulus ratio from the second 300 iterations was computed and significance was

assessed via 1000 phase perturbation trials. Eq. 1 models dynamics in terms of log-biomass whereas results in the main text are computed on untransformed biomasses. I therefor computed modulus ratios on  $e^{x_i(t)}$  in all cases so that results are consistent with analyses presented in the main text.

Modulus ratios simulated under scenario 1 are strongly skewed leftward towards zero. The mode occurs at roughly 0.25. The skew towards smaller values is nothing more than a reflection of the well known portfolio effect<sup>6</sup> which causes an overall reduction in total biomass variation with increasing numbers of species in a community. The portfolio effect occurs even though species fluctuate independently. A consequence of the portfolio effect is that it becomes harder to distinguish genuine compensation from random effects as the number of species grows. The simulations indicate that compensation beyond the portfolio effect corresponds to modulus ratios approaching zero. Near zero, the phase perturbation method exhibits a high detection rate indicating good statistical power. Detection rates are similarly high for large modulus ratios rapidly switching from 0 to 1 at around a modulus ratio of 0.6. (In terms of  $\kappa$ , detection rate jumps rapidly from approximately 0 to approximately 1 at between  $\kappa = 0.1$  and  $\kappa = 1.0$ .) The relatively large span over which detection rates are zero implies that it is exceedingly unlikely reject the null in favor of synchrony when in fact the dynamics are compensatory (an vice versa). Overall, the results indicate that the phase perturbation method is robust to spurious conclusions and exhibits high statistical power when patterns are indeed present in the data.

**Influence of zeros.** Many time series methods can be influenced by the presence of zeros in data. I examined the effect of zeros on the modulus ratio by simulating time series according to Eq. 1 and then replacing the smallest 50% of values with zeros. The truncation was computed after exponentiation the simulation results. Parameters were as in Figure S2. Simulations were repeated 1000 times split evenly between scenarios 2 and 3. The results show that this method is relatively immune to the occurrence of zeros (Figure S3).

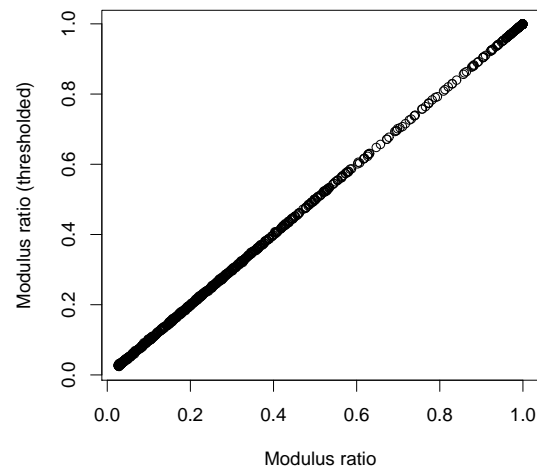


Figure S3: Comparison of modulus ratios from simulated time series with and without zero thresholding. On the X-axis are values from the original time series and on the Y-axis, modulus ratios computed on the same time series, but with the smallest 50% of values set to zero.

## References

- [1] R Development Core Team. *R: A Language and Environment for Statistical Computing*. R Foundation for Statistical Computing, Vienna, Austria, (2007). ISBN 3-900051-07-0.

- [2] Ives, A. R., Dennis, B., Cottingham, K. L., and Carpenter, S. R. Estimating community stability and ecological interactions from time-series data. *Ecological Monographs* **73**, 301–330 (2003).
- [3] Rao, J. S. and SenGupta, A. *Topics in Circular Statistics*. World Scientific, Singapore (2001).
- [4] Silverman, B. W. *Density Estimation for Statistics and Data Analysis*. Chapman and Hall, London (1986).
- [5] Loader, C. *Local Regression and Likelihood*. Statistics and Computing. Springer, New York (1999).
- [6] Doak, D., Bigger, D., Harding, E., Marvier, M., O'Malley, R., and Thomson, D. The statistical inevitability of stability-diversity relationships in community ecology. *The American Naturalist* **151**, 264–276 (1998).